

1           A Fast Seismic Assessment Technique for Reinforced  
2 Concrete Buildings: Machine Learning-based Hassan Index

3       Fahri Baran Koroglu<sup>a,b,\*</sup>, Muhammet Fethi Gullu<sup>a</sup>, Serdar Ciftci<sup>c</sup>, Liam  
4           Pledger<sup>d</sup>, Claudio Schill<sup>d</sup>, Santiago Pujol<sup>d</sup>

*<sup>a</sup>Department of Civil Engineering, Harran University, Sanliurfa, Turkiye*

*<sup>b</sup>Department of Civil Engineering, Middle East Technical University, Ankara, Turkey*

*<sup>c</sup>Department of Computer Engineering, Harran University, Sanliurfa, Turkiye*

*<sup>d</sup>Department of Civil Engineering, University of Canterbury, Christchurch, New Zealand*

---

5 **Abstract**

Assessing large inventories of reinforced concrete structures in urban areas with high seismicity is a daunting task that requires tools that can be applied quickly to produce reliable results. The first goal should be to identify the most vulnerable structures requiring fast intervention. Existing assessment standards are often too complex for this purpose. Shiga et al. [1] and Hassan and Sozen [2] have proposed more efficient assessment options based on simple geometric parameters. The question addressed here is whether machine learning (ML) algorithms trained to use the same parameters can match field observations better. Survey data from 1,320 low- and mid-rise RC buildings are used to train and test an algorithm for seismic vulnerability classification. The algorithm was able to produce modest improvements in vulnerability classification, relative to the Hassan Index and for the dataset used in its training and testing. Yet, for a separate and independent dataset, the algorithm produced nearly the same quality of results as its empirical counterpart, which can be used using simple arithmetic. Nevertheless, the exercise presented suggests that it is worth compiling more data to keep exploring the possibilities ML offers.

6 *Keywords:* Reinforced Concrete, Seismic Vulnerability, Machine Learning,  
7 Support Point Method, Rapid Assessment

---

\*Corresponding author.

*Email address:* fbkoroglu@harran.edu.tr (Fahri Baran Koroglu)

## 8 1. Introduction

9 Major earthquakes are still a serious risk to our society, as illustrated by  
10 recent earthquakes in Taiwan (2024), Türkiye (2023), Syria (2023), and Mo-  
11 rocco (2023). Although seismic design codes and guidance have improved,  
12 seismically vulnerable buildings are still the leading cause of the economic  
13 destruction and loss of lives resulting from earthquakes, and quick assess-  
14 ment of the building stock is challenging. Large cities contain thousands  
15 of buildings, and current assessment methods to estimate building seismic  
16 vulnerability often involve convoluted analyses that can often require weeks  
17 of work per building.

18 The number of buildings and the effort associated with seismic assessment  
19 today make the cost of identifying the most critical buildings in a large ur-  
20 ban area prohibitive. A less demanding alternative is to use simple building  
21 properties, easily derived from building plans or similar, to classify buildings  
22 in terms of their estimated need for strengthening. Such a pragmatic assess-  
23 ment method, if reliable, would drastically reduce the number of buildings  
24 that need to be assessed in detail.

25 A dataset of 1320 buildings surveyed after earthquake events around the  
26 world was used to train and test a machine learning (ML) model to differen-  
27 tiate between structures with and without severe damage. Damage reports  
28 and simple geometric quantities such as the number of stories, floor area,  
29 and the area of columns and walls were used to train the ML model. The  
30 model was then tested against a subset of the surveyed buildings and results  
31 were compared against results obtained using the Hassan Index [2], a more  
32 conventional assessment method used to classify vulnerable RC structures.

## 33 2. Background - RC structure vulnerability and damage classifi- 34 cation

35 Hassan and Sozen [2] proposed one of the simplest methods to classify build-  
36 ing structures according to their seismic vulnerability. Its simplicity does not  
37 detract from its reliability [3]. The data used to calibrate and test the method  
38 are open to the public and can be accessed at <https://datacenterhub.org>.  
39 The method proposed by Hassan and Sozen [2] is represented by Eq. (1). A  
40 threshold defines a boundary between the more vulnerable and less vulner-  
41 able buildings, for prioritization purposes.

$$\text{Building Status} = \begin{cases} \text{More vulnerable} & \text{if } PI < 0.25\% \\ \text{Less vulnerable} & \text{if } PI \geq 0.25\% \end{cases} \quad (1)$$

42 Here, the priority index,  $PI$ , is equal to  $CI + WI$ . The column index ( $CI$ )  
 43 is equal to half of the total cross-sectional area of reinforced concrete (RC)  
 44 columns at the base divided by the total floor area of the building above the  
 45 ground, as shown in Eq. (2). Similarly,  $WI$  represents the wall index and is  
 46 given in Eq. (3).

$$CI = \frac{A_{ct}}{2 \cdot \sum A_{ft}} \cdot 100 \quad (2)$$

$$WI = \frac{A_{wt}}{\sum A_{ft}} \cdot 100 \quad (3)$$

47  $\sum A_{ft}$  is the total floor area of the building above the ground, and  $A_{wt}$  is  
 48 the sum of the cross-sectional areas of: (a) reinforced concrete walls, and  
 49 (b) masonry infill walls, in one floorplan direction and at the base of the  
 50 building (unless a higher level is deemed more critical). Hassan and Sozen  
 51 [2] recommended dividing the term related to infill by 10.

52 The threshold on the right-hand side of Eq. (1) can be tuned depending on  
 53 local perceptions of risk and availability of resources. Buildings above the  
 54 threshold are classified as less vulnerable, and buildings below the thresh-  
 55 old are classified as more vulnerable. The qualifiers “less” and “more” are  
 56 needed because large swathes of towns often contain large numbers of build-  
 57 ings without the stiffness and the detailing needed to survive strong ground  
 58 motion. An assessment system that requires fixing everything that does not  
 59 meet current design norms often leads to inaction. The idea here is to reduce  
 60 the problem to a manageable size by focusing first on the worst cases. Fig-  
 61 ure 1 illustrates the results of reconnaissance work after the Erzincan 1992  
 62 earthquake, plotted in the manner developed by Hassan and Sozen [2]. Each  
 63 scatter point represents a building surveyed after the earthquake.

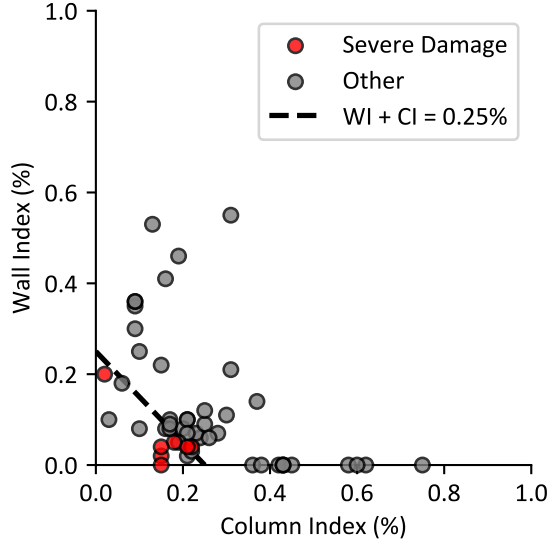


Figure 1: Relationship between column index (%), wall index (%), and reported damage to buildings after the 1992 Erzincan earthquake.

64 The exact shape or slope of the threshold in Eq. (1) and illustrated in Figure  
 65 1 does not appear to have a clear and direct impact on the balance between  
 66 cost and benefits associated with using the classification method[4]. A more  
 67 stringent threshold can help identify more critically vulnerable buildings,  
 68 but it can also misclassify more buildings that may not require urgent in-  
 69 tervention. At the same time, avoiding unnecessary retrofits by using a less  
 70 stringent threshold results in a greater number of vulnerable buildings not  
 71 classified as such.

72 The ideal classification method should minimize the number of misclassifi-  
 73 cations. The probability of misclassification is assessed using existing survey  
 74 data. To organize the available data, two types of misclassifications are  
 75 considered:

- 76 • **False Negative:** A building observed to have **severe damage** after  
 77 an earthquake but classified as **less vulnerable**.
- 78 • **False Positive:** A building observed to **not have severe damage**  
 79 after an earthquake but classified as **more vulnerable**.

80 Here, “risk” refers to the number of false negatives, while “cost” refers to  
 81 the number of false positives. The terms “risk” and “cost” are expressed as

82 percentages of the total number of buildings, and values near zero indicate  
 83 that the seismic assessment technique is effective. Substantial risk can lead  
 84 to loss of lives, and excessive cost can lead to waste, unaffordability, and  
 85 inaction.

86 Figure 2 illustrates the terms “cost” and “risk” as red quadrants in a 2x2  
 87 graphical “confusion” matrix. The quadrants along the opposite diagonal are  
 88 related to true positives and negatives, i.e., the match between the assigned  
 89 vulnerability level and damage observed in the field. The percent of buildings  
 90 in the quadrants along this diagonal representing matching classifications and  
 91 observations can be considered a measure of the reliability of the assessment  
 92 method.

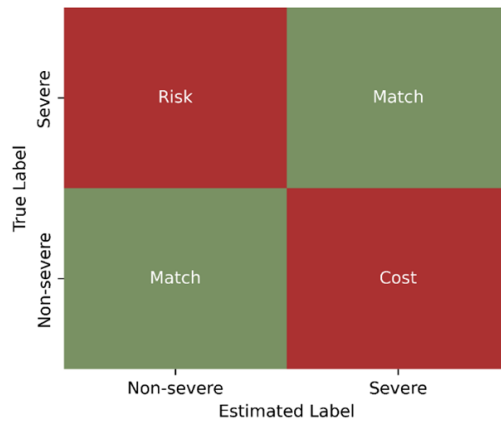


Figure 2: Definition of quadrants in confusion matrix regarding the seismic assessment classification.

93 The Hassan Index has been tested against field observations repeatedly [2–  
 94 10]. Consistently, these tests have shown a correlation between the frequency  
 95 of severe damage (presence of structural failures) and  $PI$ , with buildings rep-  
 96 resented by values of  $PI$  less than 0.1% classified as having “severe damage”  
 97 in nearly 2 out of every 3 studied cases. Care must also be taken when as-  
 98 ssuming structures that did not sustain severe damage. The words of Howe  
 99 [11] should be kept in mind: “Merely because a building has escaped injury  
 100 in an earthquake is no guarantee that it is earthquake proof. One can be  
 101 sure only if it is known to have the necessary strength and stiffness. It may  
 102 only have been lucky. Not every soldier who goes into battle is hit. Because

103 [they] escaped does not prove [they were] bulletproof.” There are numerous  
104 examples from previous reconnaissance efforts where seemingly poorly con-  
105 structed buildings remained undamaged or where identical buildings such as  
106 school or apartment blocks in close proximity experienced large differences  
107 in structural damage from collapse to light damage [4-6, 10, 12].

108 Nevertheless, the point can still be made that too many buildings with low  
109 values of  $PI$  have been reported not to have experienced severe damage  
110 in zones inferred to have experienced intense ground motion. Reducing the  
111 number of false negatives (“cost”), may help redirect scarce resources required  
112 for strengthening.

113 The goal of this study is to use machine learning to try and organize the avail-  
114 able field data better, reducing the number of misclassifications. In order to  
115 achieve the proposed aim, this is a leading and novel paper in the sense of  
116 estimating the seismic vulnerability of reinforced concrete buildings by com-  
117 bining an existing assessment method and deep neural networks, evaluating  
118 the reliability of the developed ML-based method from the perspective of  
119 risk and cost terms, utilizing a more appropriate splitting technique for the  
120 dataset. On top of these, the performance of the developed ML-based model  
121 is proven in the field by the data from the Taiwan earthquake [13].

### 122 **3. Surveyed data description**

123 Survey data from various regions of the world, ranging from Ecuador [9] to  
124 Taiwan [3], was compiled to calibrate and test a machine learning model.  
125 The surveyed data include eight input parameters, or features, that were  
126 used to train, validate, and test the ML model:

- 127 1. The number of floors of the building,
- 128 2. The typical floor area of the building,
- 129 3. The total floor area of the building above the ground,
- 130 4. The total cross-sectional area of RC columns in the first floor,
- 131 5. The total cross-sectional area of RC walls in the NS direction of the  
132 floor plan,
- 133 6. The total cross-sectional area of RC walls in the EW direction of the  
134 floor plan,
- 135 7. The total cross-sectional area of masonry infill in the NS direction of  
136 the floor plan,
- 137 8. The total cross-sectional area of masonry infill in the EW direction of  
138 the floor plan.

139 These features can be easily derived from building floor plans (formal or  
 140 sketched in the field). Figure 3 shows an example of a form used in the field  
 141 to collect information about a particular building.

142 The compiled dataset classifies each surveyed building into one of five dam-  
 143 age classes according to what was observed in the field: “None”, “Light”,  
 144 “Moderate”, “Severe”, and “Collapse”, as defined in [6]. Nevertheless, for sim-  
 145 plicity, the damage classes were grouped into two classes: “Non-severe” and  
 146 “Severe” damage. The non-severe damage class includes surveyed buildings  
 147 that experienced no damage, light, or moderate damage. The severe damage  
 148 class contains cases of severely damaged buildings and collapse. The dam-  
 149 age class of each surveyed building is used to train, validate, and test a ML  
 150 model to classify buildings as more or less vulnerable. Section 4 describes  
 151 the ML model and the training process in detail.

GUIDANCE DOCUMENT: ACI 133 Reconnaissance Activities

Legend:

- M WALL W/ OPENING
- M SOLID INFILL WALL
- RC WALL
- RC COL.
- CAPTIVE
- SEV. DMG

TEAM: SP??  
 DATE: MARCH

BUILDING (location)

N	36	13	25.3
E	36	07	21.2
	deg	min	sec

STRUCTURE (descript.) YEAR (construct.)  
 2023

No. STORIES ABOVE GROUND  
 6 + BASEMENT

HEIGHT  
 200

PICTURE #S

DAMAGE LEVEL  
 RC Structure: M M. Walls: C

PERMANENT DRIFT

OBSERVATIONS  
 SPALLING  
 CONSTRUCTION PROBLEM ON  
 JOINT CASTING

PLAN VIEW - 1 STORY

Make sure you include:

Overhangs  Col. dims.  Captive Col.  Slott Story  Obvious Eccentricity  Retrofit  RC wall min. dim.  M wall min. dim.

Figure 3: A filled-in typical floor plan form used in reconnaissance visits to gather building data.

152 The dataset contains 1320 surveyed buildings, of which 524 were classified

153 as severely damaged in the field. A more balanced dataset would require  
154 surveying more buildings with severe damage in future reconnaissance vis-  
155 its, but it is understood that severely damaged buildings can often be a)  
156 dangerous to survey and b) abandoned and inaccessible.

157 The dataset is divided into three subsets for training, validation, and testing  
158 purposes. A method called SPlit developed by [14], based on the support  
159 points method [15], was used to partition the dataset, preserving the statisti-  
160 cal properties of the main dataset within the corresponding subsets. Table 1  
161 lists the statistical properties of parameters used in the training, validation,  
162 and test datasets. The cross-sectional area of the lateral load system and the  
163 masonry infill is normalized with respect to the total floor area to facilitate  
164 the interpretation of the numbers in the table. The parameters (or features);  
165 “Minimum Wall Index [%]”, “PI [%]”, and “PI/Number of Floors” were de-  
166 rived from ad hoc feature engineering and resulted in improved performance  
167 of the DNN model.

168 Most surveyed buildings had fewer than 6 floors. The typical floor area of  
169 the surveyed buildings was smaller than 500 square meters, and in most  
170 cases, the floor area was uniform up to the height of the building. Over  
171 90% of the surveyed structures had wall area ratios smaller than 0.2% in  
172 either direction. Findings from previous surveys highlight that buildings in  
173 Japan or Chile –which tend to have low seismic vulnerability [16, 17]– have,  
174 on average, a wall area ratio greater than 0.35% in each direction [1, 6, 18].  
175 For the full dataset of surveyed structures, the average masonry infill area  
176 ratio in either direction is approximately 0.04%, with 80 % of the structures  
177 having less than 0.1% masonry infill.

## 178 **4. Machine-Learning model development**

### 179 *4.1. Model Architecture*

180 This study employs fully connected neural networks (FCNNs) to estimate a  
181 structure’s earthquake vulnerability. This section provides a brief overview  
182 of FCNNs, followed by the model architecture and training hyperparameters  
183 used in this study. An FCNN is made up of an input layer, one or more  
184 hidden layers, and an output layer. Each layer, except for the input layer,  
185 consists of artificial neurons, each of which is fully connected to all neurons  
186 in the previous layer, as shown in Figure 4b. An artificial neuron computes  
187 a weighted sum of its inputs and applies an activation function to introduce



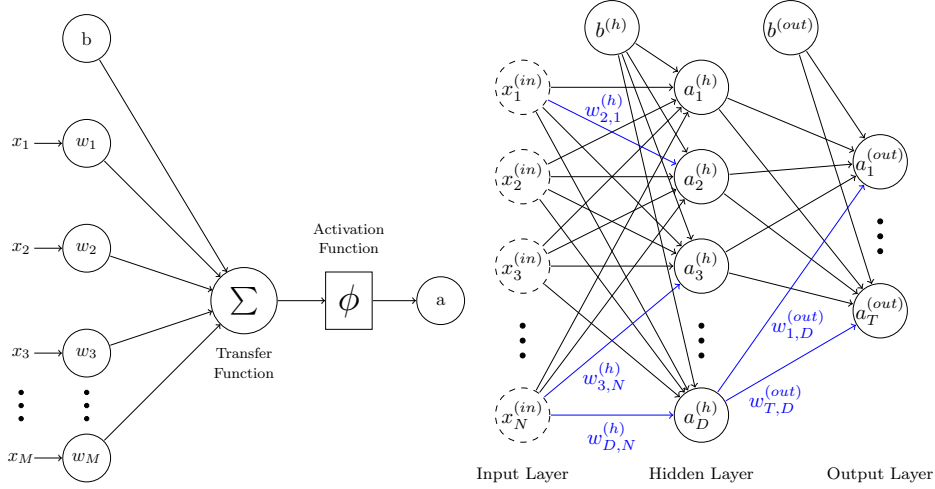


Figure 4: a) Schematic of an artificial neuron with  $M$  inputs b) Schematic of single hidden layer FCNN, with  $N$  inputs,  $D$  hidden units and  $T$  outputs.

188 nonlinearity. The output of an artificial neuron with  $M$  inputs is given by:

$$a = \phi \left( \sum_{i=1}^M w_i x_i + b \right) \quad (4)$$

189 where  $w_i$  is the weight corresponding to the  $i$ -th input  $x_i$ ,  $b$  is the bias term,  
 190 and  $\phi$  is the activation function. A schematic of an artificial neuron is shown  
 191 in Figure 4a. Forward propagation is the process of computing the FCNN's  
 192 output layer by layer, where each layer's output serves as the input for the  
 193 next. The output of the  $h$ -th layer in the FCNN is simply the activation of  
 194 each of its  $D$  artificial neurons,  $\mathbf{a}^{(h)} = [a_0^{(h)}, a_1^{(h)}, \dots, a_i^{(h)}, \dots, a_D^{(h)}]$ .

195 Training an FCNN involves optimizing the weights and bias of each neuron.  
 196 This is achieved iteratively by computing the model output, comparing it  
 197 with the desired output, and calculating the error using the loss function.  
 198 The loss function quantifies the difference between the model's predictions  
 199 and ground truth. For regression tasks, mean squared error (MSE) is com-  
 200 monly used, while cross-entropy loss is standard for classification. Once the  
 201 error is calculated, the model parameters are updated using the backprop-  
 202 agation algorithm. For further details on the training of neural networks,  
 203 refer to Chapter 6 in [19].

204 In this study, the FCNNs uses 11 inputs (see Table 1) and four hidden layers

205 containing 16, 32, 64, and 128 neurons, respectively. Leaky ReLU [20] is used  
 206 as the activation function for all neurons, except for the single neuron in the  
 207 output layer, which uses a linear activation function. Structures are then  
 208 classified as more or less vulnerable using a threshold of 0.5. Additionally,  
 209 batch normalization [21] was applied to stabilize training, and dropout [22]  
 210 (drop rate = 0.25) was used to reduce overfitting. A schematic diagram of  
 211 the model architecture is shown in Figure 5.

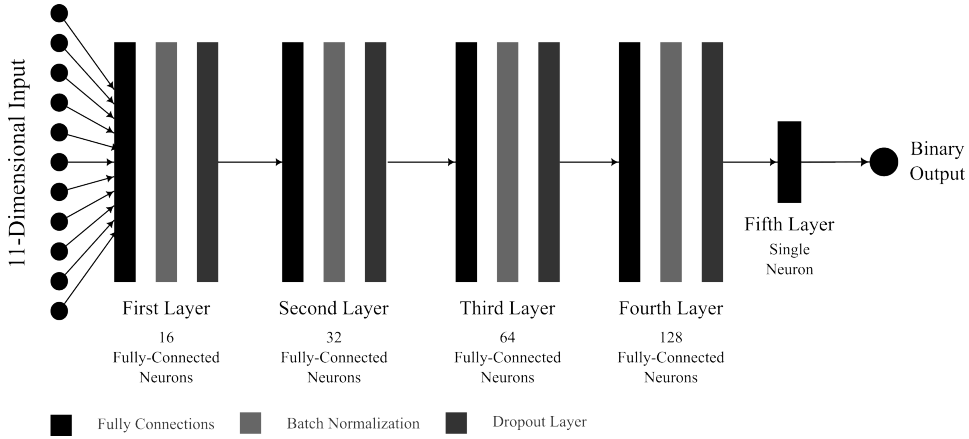


Figure 5: Implemented DNN architecture for RC building vulnerability estimation.

212 *4.2. Dataset Split, Model Training, and Performance Evaluation*

213 The full dataset is split into three different subsets called training, validation,  
 214 and test datasets. The training subset is used to calibrate the model weights  
 215 and parameters while the validation subset is used to evaluate the perfor-  
 216 mance of the model during training. Hyperparameters such as the learning  
 217 rate, dropout rate, etc., were fine-tuned based on the validation subset as  
 218 fine-tuning based on the training performance can lead to overfitting. In  
 219 order to prevent overfitting of the DNN models, three practices have been  
 220 adopted in this work:

- 221 1. Learning rate scheduler,
- 222 2. Fine-tuning of hyperparameters and performance evaluation of the  
 223 model based on the performance of the validation dataset,
- 224 3. Regularization by using dropout technique.

225 Once fine-tuning is complete on the validation subset, the test set, which  
 226 is neither used for training nor validation purposes, is used to evaluate the  
 227 final performance of the DNN without an obvious bias.

228 The full dataset is split with ratios of 72.6%, 12.8%, and 14.6% for training,  
 229 validation, and test sets, respectively. The methodology followed for the  
 230 dataset splitting and model training/evaluation for a single DNN model is  
 231 illustrated in Figure 6.

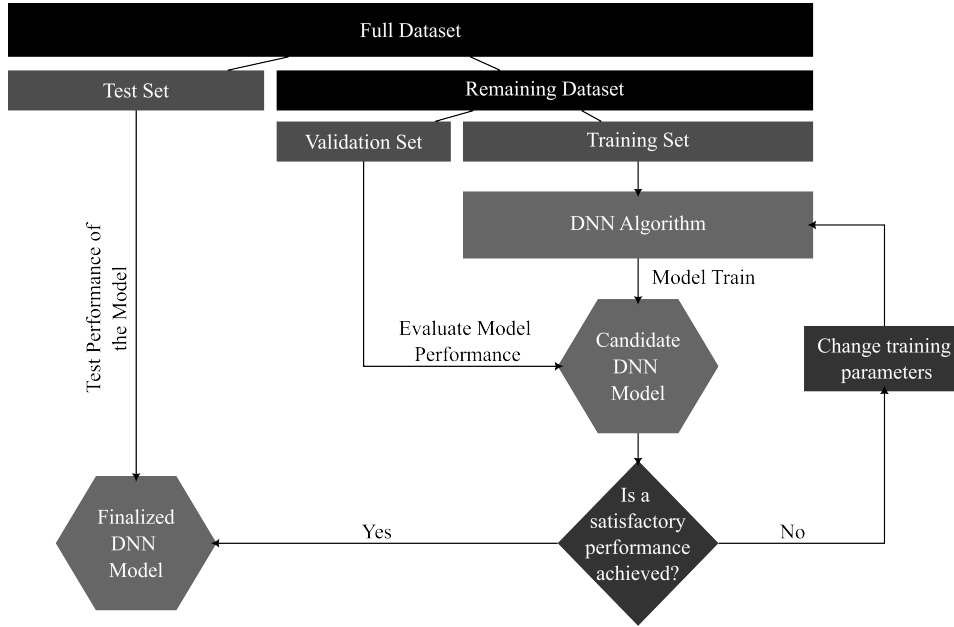


Figure 6: Flowchart of the dataset splitting and DNN model selection.

232 One of the critical parameters during the training of DNN models is the  
 233 learning rate. A high learning rate can lead to overshooting and failure  
 234 to converge to a solution. Alternatively, a low learning rate increases the  
 235 computation cost, and can lead to an underfitted model that has converged  
 236 a local minima. A learning rate drop scheduler is used to gradually reduce or  
 237 “drop” the learning rate of the model during training and avoid overfitting of  
 238 the model. DNN models can quickly overfit if the training set is small. Ad-  
 239 hoc fine-tuning of the algorithm was used in this study. During the model  
 240 training, the training and validation error histories were monitored to ensure  
 241 that the model was not overfitting.

#### 242 4.3. Handling of Imbalanced Dataset

243 The full dataset is slightly biased with 524/1320 ( 40%) of the surveyed  
 244 buildings classified as having severe damage and this bias can impact the

245 algorithm. For example, the DNN model may be more likely to classify the  
246 buildings as less vulnerable due to having a higher amount of non-severely  
247 damaged samples. Nevertheless, it is possible to prevent this by introducing  
248 a penalty factor, which has been calculated as the ratio of the total amount  
249 of non-severely damaged buildings to the severely damaged buildings. The  
250 penalty factor is used to increase the weight of the “error” during training re-  
251 lated to the misclassification of underrepresented class (in this case, severely  
252 damaged buildings).

#### 253 *4.4. DNN Senate Concept*

254 When developing a neural network, each connection between neurons has an  
255 initial weight and bias. Different initial weights can lead to a different DNN  
256 model after training. For example, one model, with certain initial weights,  
257 may classify a building as “more vulnerable”, while another model, with  
258 different initial weights, may classify the same building as “less vulnerable”.  
259 A good DNN model, with well-tuned training parameters, tends to be less  
260 receptive to changes to the initial weights. Nevertheless, cherry-picking the  
261 best-performing model carries a risk of producing formulations that perform  
262 poorly for unseen data, especially when the model is trained and validated  
263 with small datasets.

264 Rather than using a single DNN model with set initial weights, this study  
265 applies the idea of using a group or “senate” of DNN models, each with  
266 different initial weights. The average output of all of the DNN models is  
267 used to classify the seismic vulnerability of each structure. This method  
268 helps to reduce any aleatoric uncertainty associated with the model. 100  
269 DNN models with the architecture illustrated in Figure 5 were trained, each  
270 with different initial weights. The five models with the highest accuracy and  
271 lowest “risk” -as described in Section 2- were used to classify structures as  
272 more or less vulnerable. All of the results in the following sections related  
273 to the DNN model refer to an average output of the 5 models.

#### 274 *4.5. DNN-based Hassan Index Method*

275 As mentioned in Section 2, more than two thirds of surveyed buildings with  
276 a  $PI$  of less than 0.1 % were classified in the field as having “severe damage”.  
277 The DNN-based Hassan Index approach proposed in this study only uses the  
278 DNN results for structures with a  $PI \geq 0.1$  % and classifies all structures  
279 with a  $PI$  of less than 0.1 % as vulnerable.

280 *4.6. Limitations and Reproducibility*

281 The ML model developed in this study was trained on a dataset of building  
282 parameters with certain statistical ranges described in Table 1. Deep neural  
283 networks have no extrapolation capacity, and results from the DNN model  
284 are not applicable for buildings that fall outside of the ranges of the defined  
285 statistical properties.

286 Different CPUs and GPUs or package versions can converge to different  
287 model parameters for a DNN due to differences in numerical precision. There-  
288 fore, it is not guaranteed that the same results can be reproducible for a  
289 DNN model in different local machines or online environments because of  
290 the possibility of being assigned to different CPUs in different logins. A  
291 Google Colab link has been created, including the trained DNN model to  
292 provide users with reproducible results regardless of the capabilities of local  
293 machines.

294 **5. Results**

295 The trained DNN model was used to classify the vulnerability of structures  
296 in the validation and test datasets. The DNN-based model results, in terms  
297 of overall accuracy and the percentage of true positives, true negatives, false  
298 positives (“cost”), and false negatives (“risk”) are shown in Table 2. The  
299 results of the DNN-based model are compared with results obtained from  
300 the Hassan Index classification method described in Section 2 along with  
301 two variants of the Hassan Index method proposed by Ozcebe et. al [23] &  
302 Shah et al. [7]. The results of the various methods are shown in Table 2.

303 The DNN-based model outperforms the Hassan Index with better overall  
304 accuracy (74% vs 61% for the test subset), and also leads to a reduced “cost”  
305 and a reduced “risk”. The similarity between the validation and test results of  
306 the DNN-based model demonstrates that the model has learned underlying  
307 trends and patterns within the dataset and provides reassurance that the  
308 model is not overfitting.

309 The formulations proposed by Ozcebe et al. [23] & Shah et al. [7] have the  
310 lowest accuracy, close to 50%, however, they also lead to the lowest “risk”  
311 or the number of false negatives at 2-3 %. While both of these formulations  
312 lead to a low “risk”, they do so by being highly conservative with a “cost” of  
313 approximately 45 %, more than double that of the DNN-based model. This  
314 high “cost” would require many buildings to be retrofitted and classified  
315 as more vulnerable even though many of these buildings were not severely

316 damaged after an earthquake. A high “cost” makes the classification method  
317 unfeasible to implement in practice and difficult to decide which building to  
318 prioritize.

319 The DNN-based model leads to the lowest value of “cost” while also keeping  
320 the “risk” low, at 5%.

### 321 *5.1. 2024 Taiwan Earthquake*

322 The Taiwan Earthquake on April 3rd, 2024 provided a perfect opportunity  
323 to test the DNN-based model against an entirely new dataset not included in  
324 the initial training, testing, or development of the model. The data collected  
325 by Shegay et al. [13] was used to test the DNN-based model. The full dataset  
326 consisted of 66 RC buildings, however, 3 of the samples were eliminated since  
327 they fell outside the statistical bounds of the model training set. Full details  
328 about the dataset are described in Shegay et al. (2025) [13]. Table 3 shows  
329 the DNN-based model results for the 2024 Taiwan Earthquake dataset along  
330 with the Hassan Index and the indices proposed by Ozcebe et al. [23] &  
331 Shah et al. [7].

332 For the Taiwan dataset, the DNN-based model has an accuracy of 73%, a  
333 “cost” of 24% and 3% “risk”. The similarity between the DNN-based model  
334 results for the Taiwan dataset, and the test and validation sets emphasize  
335 that the model is not overfitting and capable of producing reliable results  
336 for new data.

337 Nevertheless, the Hassan Index leads to the same level of accuracy from the  
338 Taiwan dataset (73%) and has a “risk” of 0%. That is, the Hassan Index  
339 threshold correctly identifies all of the severely damaged structures surveyed  
340 in Taiwan. The “cost” is 27%, slightly higher than the DNN model. The  
341 results suggest that the Hassan Index is as effective as the DNN model in  
342 the case of surveyed buildings in Taiwan.

343 The Hassan Index variations proposed by Ozcebe et al. [23] & Shah et al. [7]  
344 have slightly lower accuracy and a larger number of false positives (“cost”)  
345 than the DNN-based model. Both formulations lead to 0% risk, the same as  
346 the Hassan Index.

## 347 **6. Discussion and limitations**

348 Overall -and on the basis of the available data- the DNN-based model tends  
349 to produce more reliable results. Nevertheless, the proposed DNN-based  
350 model should be used to produce relative vulnerability measures. That is,

351 the method would be best used to decide which building to strengthen first  
352 instead of trying to classify some buildings as “earthquake-proof,” which is,  
353 of course, futile. In fact, it is prudent to admit that in the field data, there  
354 are abundant instances of buildings that would be deemed vulnerable to  
355 earthquakes through any objective measure that, for unclear reasons, have  
356 survived earthquakes without significant damage. In that sense, the com-  
357 plete elimination of “cost” through DNN may cause unreasonable increases  
358 in “risk.” Another potential shortcoming of the use of DNN is that it requires  
359 the use of software, while existing methods require only arithmetic. To ad-  
360 dress this problem, the ready-to-use source code of the deep neural network  
361 described and trained as explained in this article can be openly accessed via  
362 this Google Colab link.

### 363 *6.1. Why 100% accuracy is unattainable*

364 Cases demonstrating wide variations in damage among comparable buildings  
365 close to one another abound Pujol et al. [4] as mentioned in Section 2. The  
366 differences can be attributed to slight variations in strength or deformability  
367 among nominally similar but brittle buildings subjected to relatively similar  
368 demands ‘hovering’ near their thresholds. It is also plausible that some  
369 buildings benefit from foundation uplift, sliding, and rocking while others  
370 do not. Classification methods such as Hassan Index or the DNN-based  
371 model would not differentiate between two geometrically identical structures,  
372 however, dozens of identical structures in the field and within the datasets  
373 have exhibited varying quantities of damage [4, 5, 10].

374 Radical differences in the performance of comparable buildings have also  
375 been attributed to plausible sharp variations in ground motion occurring  
376 within relatively short distances [12]. This study does not explore the effects  
377 of varying ground motion intensity on the likelihood of damage, and only  
378 considers geometrical properties. Some of the surveyed cities had few or no  
379 accelerometers nearby to record the ground shaking, for example: Hassan  
380 and Sozen [2]. Additionally, the intensity of shaking varied widely among  
381 the different surveys, with a recorded peak ground velocity (PGV) of nearly  
382 200 cm/s in Türkiye (2023), and a PGV of approximately 40 cm/s in the  
383 areas surveyed after the 2016 Taiwan earthquake.

384 As mentioned in Section 2, these classification methods employ simple ge-  
385 ometrical properties of the structure and do not consider aspects such as,  
386 the age of the building, construction quality, detailing of reinforcement, the  
387 location of lap splices, concrete cover, or the layout of the lateral load resist-  
388 ing system. Additionally, this study focuses on surveyed buildings that have

389 sustained severe damage and does not distinguish between other structures  
390 that sustained moderate, light, or no damage.

391 Because of the listed reasons, the work presented here was done understand-  
392 ing that complete elimination of false negatives, i.e., reducing “cost” to zero,  
393 may neither be possible nor desirable without detailed information about  
394 each building and the intensity of the motion imparted to the foundations  
395 of each building. From that point of view, it should be clear that reducing  
396 “risk” (i.e., reducing “false negatives”) is much more crucial than reducing  
397 cost.

### 398 *6.2. The black-box nature of machine learning and neural networks*

399 Lastly, machine learning can be perceived as a threat to the ability of the  
400 engineer to understand the mechanics of the problem at hand. At least two  
401 responses are in order: 1) mechanics remains the best means to identify  
402 parameters that can be used within machine learning algorithms, and 2)  
403 the engineer shall be required to investigate how results obtained with an  
404 ML model change with assumed variations in input parameters and judge  
405 whether the inferred variations can be justified from first principles. In short,  
406 machine learning shall not prevent thinking. In that sense, machine learning  
407 represents a new type of ‘calculator,’ not a new type of engineering.

## 408 **7. Conclusions**

409 This paper introduces a promising and fast seismic assessment technique,  
410 the DNN-based Hassan Index Method, which combines deep neural networks  
411 (DNNs) with the assessment method proposed by Hassan and Sozen [2] for  
412 reinforced concrete buildings. The performance of the proposed technique is  
413 compared with the performance of the original formulation by Hassan and  
414 Sozen [2] based on three parameters:

- 415 • **Accuracy:** The percentage of cases classified in agreement with ob-  
416 servation as less or more prone to severe damage.
- 417 • **Risk:** The percentage of false negatives, buildings that are considered  
418 “safe” but surveys show that they experienced severe damage.
- 419 • **Cost:** The percentage of false positives, buildings that are considered  
420 “more vulnerable” but surveys show that they did not experience severe  
421 damage.



422 Compared with the use of the criterion proposed by Hassan and Sozen [2],  
423 which states that  $PI \leq 0.25\%$  indicates higher vulnerability (a threshold  
424 that can and should be adjusted depending on local conditions and risk  
425 tolerance), the use of the DNN-based method helped:

- 426 1. Increase **accuracy** by a factor of 1.25 for the test set (from approxi-  
427 mately 61% to 75%),
- 428 2. Reduce **cost** by a factor of 1.50 for the test set (from approximately  
429 31% to 20%), and
- 430 3. Decrease **risk** by factor of 1.50 (from 8% to 5%).

431 The caveats presented in Section 2 and Section 6.1 about apparently vul-  
432 nerable buildings that have been observed to survive earthquakes should be  
433 kept in mind in relation to **3**. It could be argued that the decrease in “**risk**”  
434 implies a potential reduction in loss of life compared with what can be ob-  
435 tained from the simple arithmetic used to compute the index proposed by  
436 Hassan and Sozen [2]. At the same time, the reduction in “**cost**” may rep-  
437 resent an opportunity to use resources more effectively. Nevertheless, given  
438 all the variables left out of the studied formulations, it is prudent to use the  
439 proposed technique to prioritize building strengthening efforts or to schedule  
440 structures for a more detailed study. As a result, a lower bound of  $PI < 0.1\%$   
441 is proposed to identify vulnerable structures, irrespective of the output from  
442 the DNN model.

443 The results show that the formulated DNN-based model has potential as  
444 an initial seismic assessment tool that can help prioritize mitigation efforts.  
445 Nevertheless, despite large increases in computational effort, only modest in-  
446 creases in performance were obtained from DNN in comparison with simpler  
447 prioritization tools. That result should not surprise given

- 448 1. the complexity of the earthquake problem,
- 449 2. the simplicity of the information available,
- 450 3. the limited number of cases with which we operate.

451 It is possible, however, that concerted efforts to collect more data will lead to  
452 improvements in the studied classification method. DNN-based algorithms  
453 work best if trained with large amounts of data. DNN algorithms trained  
454 using small datasets are prone to “overfitting”. In this study, overfitting  
455 was kept in check by using the “dropout” technique and the “learning-rate  
456 scheduler”, Nevertheless, the results presented suggest that use of DNN in  
457 seismic assessment still needs to be guided by experience and engineering  
458 judgment.

459 The data and codes used in this study have been made public to benefit gov-  
460 ernmental institutions and industry. The proposed technique’s applicability  
461 should be restricted to conditions similar to those in which the data used for  
462 calibration were collected.

### 463 **Acknowledgement**

464 The authors greatly acknowledge the efforts of those who surveyed and gath-  
465 ered the data after previous earthquakes.

### 466 **References**

- 467 [1] T. Shiga, Earthquake damage and wall index of reinforced concrete  
468 buildings, Architectural Institute of Japan (1968) 29–32.
- 469 [2] A. F. Hassan, M. A. Sozen, Seismic vulnerability assessment of low-  
470 rise buildings in regions with infrequent earthquakes, *ACI Structural*  
471 *Journal* 94 (1997) 31–39.
- 472 [3] A. Y. Puranam, A. Irfanoglu, S. Pujol, T. C. Chiou, S. J. Hwang, Eval-  
473 uation of seismic vulnerability screening indices using data from the  
474 taiwan earthquake of 6 february 2016, *Bulletin of Earthquake Engineer-*  
475 *ing* 17 (2019) 1963–1981.
- 476 [4] S. Pujol, L. Laughery, A. Puranam, P. Hesam, L. H. Cheng, A. Lund,  
477 A. Irfanoglu, Evaluation of seismic vulnerability indices for low-rise re-  
478 inforced concrete buildings including data from the 6 february 2016  
479 taiwan earthquake, *Journal of Disaster Research* 15 (2020) 9–19.
- 480 [5] C. Dönmez, S. Pujol, Spatial distribution of damage caused by the 1999  
481 earthquakes in turkey, *Earthquake Spectra* 21 (2005) 53–69.
- 482 [6] S. Pujol, I. Bedirhanoglu, C. Donmez, J. D. Dowingala, M. Eryilmaz-  
483 Yildirim, K. Klaboe, F. B. Koroglu, R. D. Lequesne, B. Ozturk,  
484 L. Pledger, E. Sonmez, Quantitative evaluation of the damage to rc  
485 buildings caused by the 2023 southeast turkey earthquake sequence,  
486 *Earthquake Spectra* 40 (2024) 505–530.
- 487 [7] P. Shah, S. Pujol, M. Kreger, A. Irfanoglu, 2015 nepal earthquake, *Con-*  
488 *crete International* 39 (2017) 42–49.

- 489 [8] C. Sim, C. Song, N. R. Skok, A. Irfanoglu, S. Pujol, M. Sozen,  
490 Database of low-rise reinforced concrete buildings with earthquake dam-  
491 age, <https://datacenterhub.org/resources/> (2016).
- 492 [9] E. Villalobos, C. Sim, J. P. Smith-Pardo, P. Rojas, S. Pujol, M. E.  
493 Kreger, The 16 april 2016 ecuador earthquake damage assessment sur-  
494 vey, *Earthquake Spectra* (2018) 1201–1217.
- 495 [10] W. Zhou, W. Zheng, S. Pujol, Seismic vulnerability of reinforced con-  
496 crete structures affected by the 2008 wenchuan earthquake, *Bulletin of*  
497 *Earthquake Engineering* 11 (2013) 2079–2104.
- 498 [11] G. E. Howe, Requirements for buildings to resist earthquakes, American  
499 Institute of Steel Construction (1936).
- 500 [12] S. Alcocer, A. Behrouzi, S. Brena, K. J Elwood, A. Irfanoglu, M. Kreger,  
501 R. Lequesne, G. Mosqueda, S. Pujol, A. Puranam, et al., Observations  
502 about the seismic response of rc buildings in mexico city, *Earthquake*  
503 *Spectra* 36 (2020) 154–174.
- 504 [13] A. Shegay, T. Suzuki, T.-C. Chiou, L. Hogan, J. Monical, H. Aydogdu,  
505 Z. Yi, J. Byrne, K. Elwood, S.-J. Hwang, K. Jiang, S.-J. Jhuang, H.-J.  
506 Lee, J.-K. Lee, C.-C. Lin, M.-L. Lin, Y.-C. Ling, H. Liu, M. Maeda,  
507 M. Otani, W.-C. Shen, D. Shearer, H. Shoda, L.-W. Song, M. Stephens,  
508 P.-W. Weng, T.-P. Yuen, C.-H. Yang, C.-H. Yang, J.-H. Zhang, Y.-  
509 J. Zeng, 2024 hualien earthquake reconnaissance of reinforced concrete  
510 buildings, Tech. Rep. NCREE-25-XXX, National Center for Research  
511 on Earthquake Engineering, Taiwan (2025, Preprint).
- 512 [14] V. R. Joseph, A. Vakayil, Split: An optimal method for data splitting,  
513 *Technometrics* 64 (2022) 166–176.
- 514 [15] S. Mak, V. R. Joseph, Support points, *The Annals of Statistics* 46 (2018)  
515 2562–2592.
- 516 [16] R. Riddell, S. L. Wood, J. C. de la Llera, The 1985 chile earthquake:  
517 Structural characteristics and damage statistics for the building inven-  
518 tory in viña del mar, *Civil Engineering Studies SRS-534* (1987).
- 519 [17] M. Sarrafzadeh, K. J. Elwood, R. P. Dhakal, H. Ferner, D. Pettinga,  
520 M. Stannard, M. Maeda, Y. Nakano, T. Mukai, T. Koike, Performance  
521 of reinforced concrete buildings in the 2016 kumamoto earthquakes and  
522 seismic design in japan, *Bulletin of the New Zealand Society for Earth-*  
523 *quake Engineering* 50 (2017) 394–435.

- 524 [18] L. Pledger, S. Pujol, R. Chandramohan, Investigating the effect of stiff-  
525 ness on the seismic performance of rc structures, in: NZSEE 2023  
526 Annual Conference, New Zealand Society for Earthquake Engineering,  
527 Auckland, New Zealand, 2023.
- 528 [19] S. Raschka, Y. Liu, V. Mirjalili, Machine Learning with PyTorch and  
529 Scikit-Learn, Packt Publishing, Birmingham, UK, 2022.
- 530 [20] A. L. Maas, A. Y. Hannun, A. Y. Ng, et al., Rectifier nonlinearities im-  
531 prove neural network acoustic models, in: Proc. icml, Vol. 30, Atlanta,  
532 GA, 2013, p. 3.
- 533 [21] S. Ioffe, C. Szegedy, Batch normalization: Accelerating deep network  
534 training by reducing internal covariate shift, in: Proceedings of the  
535 32nd International Conference on Machine Learning, 2015.
- 536 [22] N. Srivastava, G. Hinton, A. Krizhevsky, R. Salakhutdinov, Dropout:  
537 A simple way to prevent neural networks from overfitting, Journal of  
538 Machine Learning Research 15 (2014) 1929–1958.
- 539 [23] G. Özcebe, J. Ramirez, S. T. Wasti, 1 may 2003 bingol earthquake - engi-  
540 neering report, <http://www.seru.metu.edu.tr/archives.html>  
541 <http://www.anatolianquake.org> (2003).

Table 1: Statistical Summary of Building Features

<b>Feature</b>	<b>Dataset</b>	<b>Min</b>	<b>Max</b>	<b><math>\mu</math></b>	<b><math>\sigma</math></b>
Number of Floors	Training	0.5	16	4.22	2.42
	Validation	1	15	4.24	2.50
	Test	1	16	4.26	2.57
Typical Floor Area [m <sup>2</sup> ]	Training	22	4880	336	322
	Validation	37	1450	330	270
	Test	35	2070	321	282
Total Floor Area [m <sup>2</sup> ]	Training	46	24400	1600	2090
	Validation	86	13400	1610	2020
	Test	52	16400	1590	2100
Column Area Ratio [%]	Training	0	2.35	0.39	0.26
	Validation	0	1.61	0.39	0.24
	Test	0	1.70	0.39	0.25
RC Wall Area Ratio (NS) [%]	Training	0	1.66	0.07	0.16
	Validation	0	1.39	0.07	0.18
	Test	0	1.39	0.07	0.16
RC Wall Area Ratio (EW) [%]	Training	0	1.52	0.06	0.14
	Validation	0	1.05	0.06	0.15
	Test	0	1.14	0.06	0.14
Masonry Infill Area Ratio (NS) [%]	Training	0	0.40	0.04	0.06
	Validation	0	0.38	0.04	0.06
	Test	0	0.33	0.04	0.06
Masonry Infill Area Ratio (EW) [%]	Training	0	0.70	0.04	0.06
	Validation	0	0.48	0.04	0.06
	Test	0	0.54	0.04	0.06
Minimum Wall Index [%]	Training	0	1.12	0.06	0.09
	Validation	0	1.05	0.06	0.10
	Test	0	0.71	0.06	0.09
PI [%]	Training	0	1.29	0.25	0.15
	Validation	0	1.05	0.25	0.15
	Test	0	1.15	0.25	0.16
PI/Number of Floors [%]	Training	0	1.78	0.10	0.14
	Validation	0	0.88	0.10	0.12
	Test	0	0.94	0.10	0.13

Table 2: Results for structural damage classification based on Hassan Index and the proposed DNN model (TP = True positive, TN = True negative, FP = False psotive, FN = False negative).

	Dataset	Accuracy	TP	TN	FP “Cost”	FN “Risk”
<b>DNN-based model</b>	Validation	75%	40%	35%	20%	5%
	Test	74%	40%	34%	21%	5%
<b>Hassan Index [2]</b>	Validation	63%	31%	32%	30%	8%
	Test	61%	30%	31%	31%	8%
<b>Ozcebe et al. [23]</b>	Validation	50%	37%	13%	47%	2%
	Test	53%	38%	15%	46%	2%
<b>Shah et al. [7]</b>	Validation	53%	37%	16%	44%	3%
	Test	52%	36%	16%	45%	3%

Table 3: Results for structural damage classification of buildings surveyed after the 2024 Taiwan Earthquake (TP = True positive, TN = True negative, FP = False positive, FN = False negative).

	Accuracy	TP	TN	FP “Cost”	FN “Risk”
<b>DNN-based model</b>	73%	44%	29%	24%	3%
<b>Hassan Index [2]</b>	73%	48%	25%	27%	0%
<b>Ozcebe et al. [23]</b>	67%	48%	19%	33%	0%
<b>Shah et al. [7]</b>	70%	48%	22%	30%	0%